

PCCP

Accepted Manuscript



This is an *Accepted Manuscript*, which has been through the Royal Society of Chemistry peer review process and has been accepted for publication.

Accepted Manuscripts are published online shortly after acceptance, before technical editing, formatting and proof reading. Using this free service, authors can make their results available to the community, in citable form, before we publish the edited article. We will replace this *Accepted Manuscript* with the edited and formatted *Advance Article* as soon as it is available.

You can find more information about *Accepted Manuscripts* in the [Information for Authors](#).

Please note that technical editing may introduce minor changes to the text and/or graphics, which may alter content. The journal's standard [Terms & Conditions](#) and the [Ethical guidelines](#) still apply. In no event shall the Royal Society of Chemistry be held responsible for any errors or omissions in this *Accepted Manuscript* or any consequences arising from the use of any information it contains.

Complex borides based on AlLiB_{14} crystal structure as high-temperature thermoelectric compounds

L. F. Wan,^{a,b} and S. P. Beckman,^{*a‡}

Received Xth XXXXXXXXXXXX 20XX, Accepted Xth XXXXXXXXXXXX 20XX

First published on the web Xth XXXXXXXXXXXX 200X

DOI: 10.1039/b000000x

AlLiB_{14} crystal is examined as a potential high-temperature thermoelectric material. First-principles methods are used to investigate the thermoelectric behavior and it is found to have a band gap of 2.13 eV, and an electronic dispersion with characteristic indicative of having a high Seebeck coefficient. Semiclassical Boltzmann transport theory predicts that AlLiB_{14} will have a Seebeck coefficient greater than $200 \mu\text{V/K}$, at temperatures near 1000 K and carrier concentrations around $1 \times 10^{20} \text{cm}^{-3}$. Using an elasticity based expression for the thermal conductivity, the thermoelectric figure of merit is approximated to be $0.45 \times 10^{-3} \text{T}$ at moderate doping levels.

1 Introduction

In recent decades, thermoelectric (TE) materials have been of great interests for potential application as power generation devices and solid-state refrigerators.^{1–3} Although TE-based technologies are promising due to being emission free and having a compact size, their applicability for broad commercial deployment is limited by their relatively poor operating efficiency. This is characterized by the dimensionless figure of merit called ZT , and is related to the Seebeck coefficient, S , electric conductivity, σ , thermal conductivity, κ , and operating temperature, T , by the equation $ZT = \sigma S^2 T / \kappa$.^{4–6} Achieving a large ZT (> 2), is challenging because of the interdependence of the physical properties that yield the TE response. For example, good electrical conductivity can be achieved by introducing high doping levels, but doping the material greatly reduces the Seebeck coefficient; in addition the flow of electrons and holes carry both charge and heat, therefore σ and κ are directly proportional. The general approach to obtain a reasonable ZT involves finding an appropriate band gap semiconductor with a large Seebeck coefficient ($S > 200 \mu\text{V/K}$) and a reasonable σ / κ ratio.

A number of material systems have been proposed for use in TE devices. Compounds based on the $\text{Bi}_2\text{Te}_3/\text{Sb}_2\text{Te}_3/\text{Bi}_2\text{Se}_3$ crystal family may be useful near room temperature and have a ZT of around 1.^{7,8} The PbTe -type compounds have potential for use at slightly elevated temperatures, $T \sim 500 \text{K}$, and also have ZT values around 1.^{1,8,9} Finding good TE for the

high-temperature regime, $T > 900 \text{K}$, has been more challenging. Alloys of $\text{Si}_x\text{Ge}_{(1-x)}$ have been considered because single crystals of these compounds are known to have a good electrical conductivity and can be easily doped p- or n-type. Unfortunately, due to their high thermal conductivity and relatively low Seebeck coefficient, the typical ZT for these compounds is between 0.6 and 1.^{10,11} In addition to the relatively low TE efficiency, the compounds such as PbTe , also suffer from being dependent on toxic elements, Pb , and rare materials, Te . It is desirable to develop new TE materials that will not only have good efficiency, but also will be made from elements that are environmentally sound and plentiful.

Experimental studies have shown that many of the boron-rich borides, which have crystal structures constructed from stacking B_{12} icosahedra, have a large Seebeck coefficient.^{12–15} This is believed in part due to the layering of B_{12} icosahedra in these crystals that lowers the dimensionality of the material.^{13,16,17} These compounds are chemically stable at high temperatures and have a relatively large band gap, which allows them to maintain a high Seebeck response even at temperatures greater than 1000 K.

The class of complex boride, based on the AlLiB_{14} crystal family, has been of interest in recent years due to its unique electronic and mechanical properties.^{18–23} The crystal structure is composed of layers of B_{12} icosahedra that are arranged in a triangular lattice. The layers of icosahedra B are stacked, and between the layers reside metal atoms. Numerous metal species can occupy these sites, but here the archetypical structure AlLiB_{14} will be the focus. The B atoms are strongly covalently bonded to each other forming a rigid structure and the metal atoms contribute their valence electrons to this B -network.^{24,25} Although this compound is known to possess a number of promising properties, such as good mechanical

^a Department of Materials Science and Engineering, Iowa State University, Ames, Iowa 50011, USA

^b The Molecular Foundry, Materials Sciences Division, Lawrence Berkeley National Laboratory, Berkeley, California 94720, USA

‡ E-mail: sbeckman@iastate.edu

strength, high melting temperature, and excellent resistance to chemical corrosion, there is yet to be a systematic study of the TE properties as it relates to the electronic structure.

In this article, the electronic structure, which directly determines the physical properties of AlLiB_{14} , is studied by *ab initio* methods. The transport properties, in particular the TE behavior, are determined by applying the semi-classical Boltzmann transport theory to the calculated electronic structure.

2 Methods

The electronic structure of AlLiB_{14} is determined using the density functional theory (DFT) based approach implemented in the Quantum Espresso source code.²⁶ The exchange-correlation energy is approximated as a local functional of charge density including the local gradients (GGA).²⁷ The Vanderbilt-type ultrasoft pseudopotentials are used in place of the all electron ion potentials.²⁸ The plane-wave expansion of the wave function is truncated at 950 eV and the Brillouin zone is sampled using a $4 \times 4 \times 4$ Monkhorst-Pack mesh,²⁹ which allows the calculated forces on the ions to have an accuracy of better than 5 meV/Å. Using this method the structurally optimized AlLiB_{14} crystal has an orthorhombic lattice with dimensions $5.86 \times 10.38 \times 8.16$ Å, which agrees well with the experimental results reported in the literatures.^{18,30} Using the calculated electronic bands, the Boltzmann transport equation^{31,32} is solved within the constant relaxation time approximation as encoded in the BoltzTraP software.³³ To ensure the accuracy of the transport properties a dense k-space mesh of $30 \times 24 \times 24$ is used.

3 Results and Discussions

Previous studies agree that the electronic density of states at the band edges are dominated by the B $2p$ -states, and the metal atoms donate their valence electrons to the entire B network.^{23–25} This can also be seen in charge density plots, which demonstrate covalent bonding between B atoms and charge depletion around the metal species.^{34,35} As a result, the Fermi level shifts around the band gap when changing the valency of metal species. However, in order to understand the transport behavior of the crystal, a more detailed analysis of the Kohn-Sham eigenstates is required. The energy bands for AlLiB_{14} are plotted in figure 1. It is found to have an indirect gap with the valence band maximum at the Γ point and the conduction band minimum along Γ -X branch. The bands near the band gap suggest that the TE response in this material will be large.^{7,36} A mixture of bands with light and heavy effective charge carriers are observed at both the valence and conduction band edges. Quantitatively, this tends to simultaneously increase the Seebeck coefficient and maintain large group ve-

locity.³⁶ The complex interaction between the B atoms also leads to a multi-valley band structure. The near equienergetic extremum are distributed across the Brillouin zone, providing charge carriers with low effective masses and non-zero lattice momentums due to this band structure.

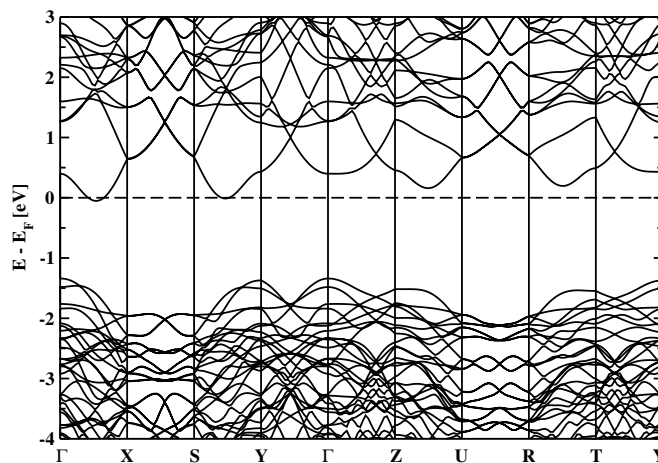


Fig. 1 The electronic band structure of AlLiB_{14} plotted along high-symmetry paths in the first Brillouin zone. The energy zero is set at the Fermi level.

Although DFT with GGA generally does an excellent job describing the ground state properties of solids, such as the bond strengths and structures, it is known to predict incorrect band gaps. To obtain a better prediction of the band gap energy the hybrid functional developed by Heyd, Scuseria and Ernzerhof (HSE) is used for the exchange-correlation energy.³⁷ Whereas DFT with GGA predicts a band gap of 1.3 eV the HSE functional returns a gap of 2.1 eV. The general shape of the DOS is the same for both the GGA and HSE functionals, which validates the shape of the bands in figure 1, although the scissor operator is needed to correct the gap. Having the correct band gap is important for accurately predicting the TE behavior, because a narrowed gap will result in bipolar conduction at low temperatures.

Werheit *et al.* have measured the absorption spectrum and report that the strongest absorption occurs at 1.95 eV, which agrees with the DFT-HSE results to within 10% and further verifies this approach.⁴¹ Our calculation suggests that the absorption events reported at lower energies are not due to inter-band transitions and are possibly due to the Urbach tails and deep states in the gap that are discussed in detail in the literature.⁴¹ Interestingly, having a band gap near 2 eV places the absorption edge in the middle of the solar spectrum, which

*In this work, the HSE functional calculation is performed using VASP.^{38–40} For the ion potentials, the projector augmented wave method is used. The results are fully converged for a 318.6 eV cutoff energy and a $6 \times 6 \times 4$ k-point sampling. The resulting band gap is around 2.12 eV.

suggests that there may be applications for this compound involving the absorption of sunlight.

Here, the Kohn-Sham eigenvalues are first calculated using the PW91-GGA functional in Quantum Espresso. The obtained eigen-energies are then used as inputs to approximate the transport behavior using BoltzTraP, where a scissor operator is applied to open the band gap from 1.3 to 2.1 eV. In figure 2, the various of transport quantities are presented as a function of the charge carrier chemical potential, μ , at $T = 1000$ K. The Seebeck coefficient is shown in figure 2(a), the electrical conductivity, σ , is given in frame (b), and the power factor, $PF = S^2\sigma$, is presented in (c). The anisotropic nature of this crystal is manifest in the TE properties with the PF differing by as much as 50% for different orientations. This is primarily due to variation in the conductivity.

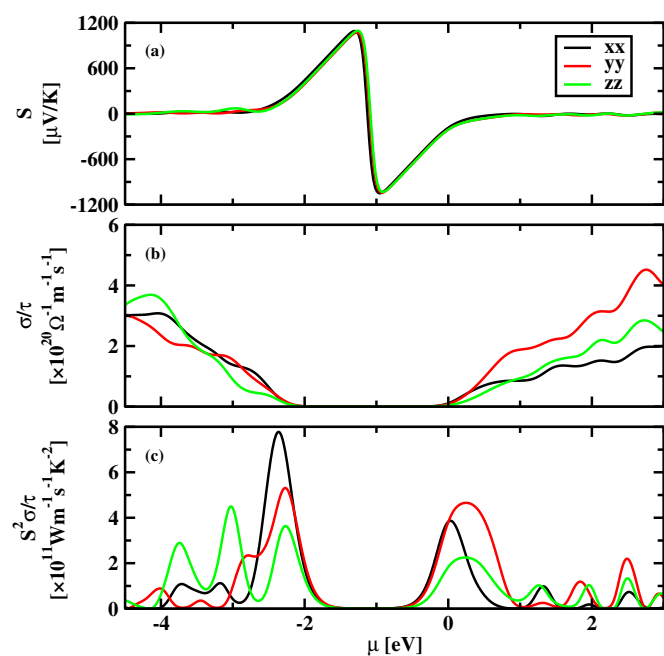


Fig. 2 The transport properties of AlLiB_{14} predicted from the electronic band structure and the Boltzmann equation. Frame (a) shows the thermopower, S , frame (b) the electrical conductivity, σ/τ , and frame (c) the power factor, $S^2\sigma/\tau$, as a function of electron chemical potential, μ , at $T = 1000$ K. The chemical potential zero is set to be the Fermi energy at $T = 0$ K. To generalize the results, the value of σ is scaled by the relaxation time for scattering events, τ .

The best TE performance is found when the chemical potential is around 1 eV below the valence band edge and 0.5 eV above the conduction band edge. Although for many crystals achieving this degree of doping may be challenging, it is known from the recent work of Maruyama *et al.* that these complex borides can be strongly doped,¹⁵ although this contradicts recent theoretical predictions.⁴² Because both the

electron- and hole-type transport behaviors are potentially important for this crystal family and the impact of carrier concentration and temperature on S are presented in figure 3. The thermopower, S , is plotted as a function of p- and n-doping levels that range from 10^{17} to 10^{21} cm^{-3} in frames (a) and (c) of figure 3. This data is rearranged to demonstrate the influence of temperature on S in frames (b) and (d) of figure 3. It is observed that the influence of doping the carrier concentration is much greater than temperature; at $n(p) = 10^{19}$ cm^{-3} , S only increases by approximately 100 $\mu\text{V/K}$ when T increases from room-temperature to 1000 K. Even though the thermopower decreases as the doping level increases, at high temperatures S is still larger than 200 $\mu\text{V/K}$. This holds even at carrier concentrations as large as 10^{20} cm^{-3} . This is due to the large band gap of AlLiB_{14} that allows for single carrier conduction to continue even at high temperatures. In contrast narrow band gap materials, such as Bi_2Te_3 and PbTe , will often experience bipolar conduction due to the simultaneous contribution of both electrons and holes to the transport process.^{9,43}

In figure 4, the PF is plotted for electron and hole carrier concentrations ranging from 10^{18} to 10^{21} cm^{-3} for a series of temperatures. The crystallographic orientation is taken into account with the first column showing the x -direction, the next showing the y -direction, and the right column showing the z -direction. Although these results predict an extremely large PF , greater than 8×10^{11} $\text{Wm}^{-1}\text{s}^{-1}\text{K}^{-2}$, for p -type conduction in the x -direction, the doping levels required to achieve this are extremely high, around 10^{21} cm^{-3} . Realistic doping levels will likely result in a more modest PF that is in the neighborhood of 1×10^{11} $\text{Wm}^{-1}\text{s}^{-1}\text{K}^{-2}$. For a charge carrier relaxation time on the order of 1×10^{-14} s this will yield a PF of 1×10^{-3} $\text{Wm}^{-1}\text{K}^{-2}$.

To complete the discussion of TE performance of AlLiB_{14} , knowledge about the thermal conductivity is needed, which is a challenging property to predict purely from first-principles methods. Clarke has proposed a classical model⁴⁴ to approximate the minimum thermal conductivity at high temperatures, κ_{min} , using

$$\kappa_{\text{min}} = k_{\text{B}} v_m \left(\frac{M}{n\rho N_{\text{A}}} \right)^{-\frac{2}{3}}$$

where

$$v_m = \left[\frac{1}{3} \left(\frac{2}{v_t^3} + \frac{1}{v_l^3} \right) \right]^{-\frac{1}{3}}$$

Here, k_{B} is the Boltzmann constant, M is the molar mass, n is the number of atoms per unit cell, N_{A} is the Avogadro constant, and ρ is the density, which is 2.475 g/cm^3 for the case of AlLiB_{14} . The variables v_t and v_l are the transverse and longitudinal sound velocities, which can be approximated from the

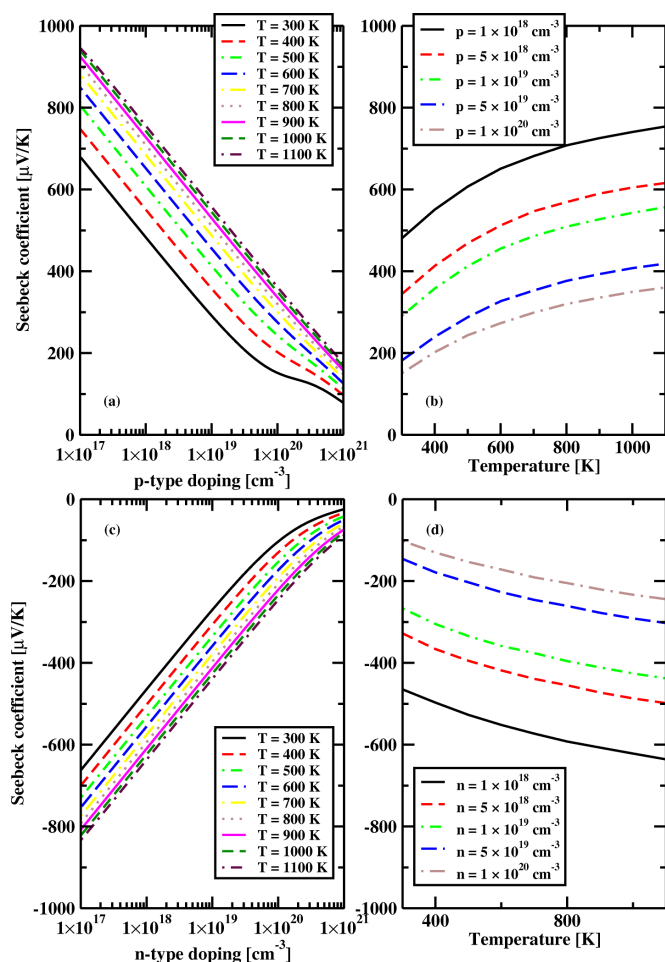


Fig. 3 The thermopower for hole- and electron-doped AlLiB_{14} , plotted as a function of carrier concentration and temperature.

averaged shear and bulk moduli

$$v_t = \sqrt{\frac{G_H}{\rho}}$$

$$v_l = \sqrt{\frac{(B_H + \frac{4}{3}G_H)}{\rho}}$$

The shear modulus, G_H , and bulk modulus, B_H , are taken from the literature⁴⁵ to be as 155 GPa and 190 GPa, which results in $\kappa_{\min} = 3.0 \text{ Wm}^{-1}\text{K}^{-1}$.

Based on the approximations of $\tau = 10^{-14} \text{ s}$ and $\kappa = 3.0 \text{ Wm}^{-1}\text{K}^{-1}$, we estimate the figure of merit ZT at $n(p) = 10^{19} \text{ cm}^{-3}$ and plot it in figure 5. Although the ZT value relies upon several approximations, it is certainly the right order of magnitude and allows for prediction of the material's limits that must be achieved. For example, from figure 5, it is determined that the a $ZT = 0.45$ can be obtained by p-doping

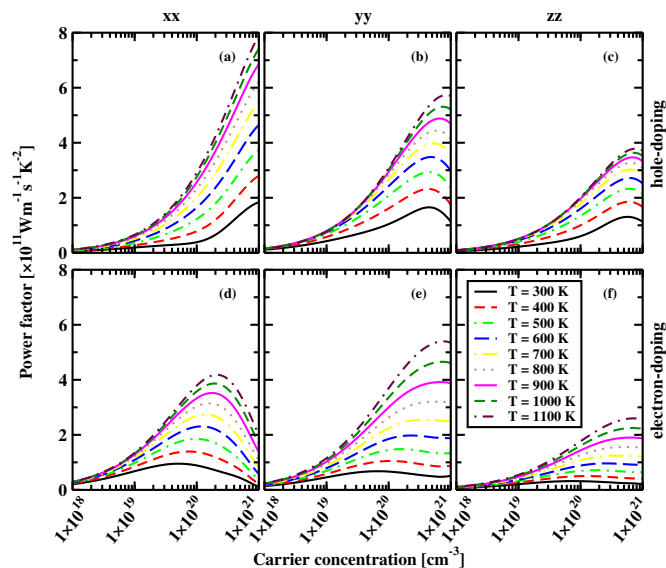


Fig. 4 The power factor, PF , for hole- and electron-doped AlLiB_{14} , plotted as a function of carrier concentration and temperature.

AlLiB_{14} at $T = 1000 \text{ K}$ at carrier concentration of 10^{19} cm^{-3} . At this time, there is no direct experimental measurements about the thermoelectric response of AlLiB_{14} , however, our predicted ZT values are comparable with other XYB_{14} compounds, such as $\text{Y}_x\text{Al}_y\text{B}_{14}$.⁴⁶

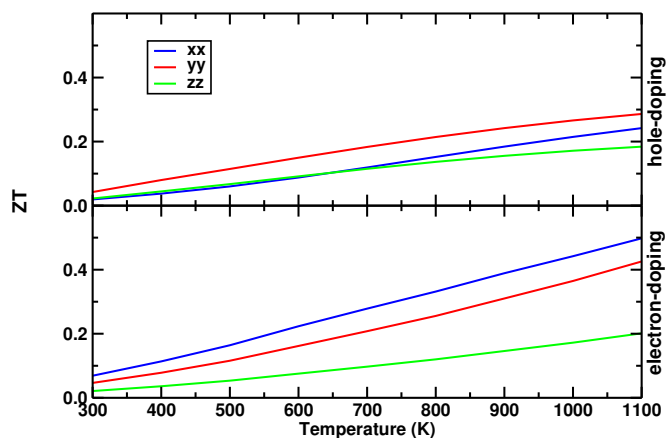


Fig. 5 The approximated figure of merit, ZT , for hole- and electron-doped AlLiB_{14} , plotted as a function of temperature at carrier concentration of 10^{19} cm^{-3} .

4 Summary

The electronic structure of AlLiB_{14} is examined in detail using density functional theory. The thermoelectric behavior of the crystal is determined by solving the Boltzmann transport

equation. The electronic band edges that determine the transport properties of AlLiB_{14} are related to the complex interactions between the B atoms. The metal atoms do not influence the states at the band edges, but instead impact the transport properties by controlling the charge carrier concentration, *i.e.*, the metal species can in principle be used to dope the boride compound. A nearly isotropic Seebeck coefficient is observed and its value maintained at larger than $200 \mu\text{V/K}$ even at extremely high doping levels. The power factor, on the other hand, is strongly orientation dependent. At $T = 1000 \text{ K}$ a power factor of $3.8 \times 10^{11} \text{ } \tau \text{ Wm}^{-1}\text{s}^{-1}\text{K}^{-2}$ is expected for carrier concentrations of 10^{20} cm^{-3} .

5 Acknowledgements

The work of LFW was sponsored in part by the US Army Research Office under contract number W911NF-11-C-0268 and in part by the National Science Foundation through grant DMR-1105641. The work of SPB was sponsored by the National Science Foundation through grant DMR-1105641.

References

- 1 *CRC handbook of thermoelectrics*, ed. D. M. Rowe, CRC Press LLC, 1995.
- 2 F. J. DiSalvo, *Science*, 1999, **285**, 703.
- 3 T. M. Tritt and M. A. Subramanian, *MRS Bull.*, 2006, **31**, 188.
- 4 *Thermoelectrics Handbook: Macro to Nano*, ed. D. M. Rowe, CRC by Taylor Francis Group, LLC, 2006.
- 5 M. S. Dresselhaus, G. Chen, M. Y. Tang, R. G. Yang, H. Lee, D. Z. Wang, Z. F. Ren, J. P. Fleurial and P. Gogna, *Adv. Mater.*, 2007, **19**, 1043.
- 6 G. S. Nolas, J. Poon and M. Kanatzidis, *MRS Bull.*, 2006, **31**, 199.
- 7 G. S. Nolas, J. Sharp and H. J. Goldsmid, *Thermoelectrics: Basic Principles and New Materials Developments*, Springer-Verlag, Berlin, 2001.
- 8 A. F. Ioffe, *Semiconductor Thermoelements and Thermoelectric Cooling*, Inforssearch, London, 1957.
- 9 C. Wood, *Rep. Prog. Phys.*, 1988, **51**, 459.
- 10 C. B. Vining, W. Laskow, J. O. Hanson, R. R. Vanderbeck and P. D. Gorsuch, *J. Appl. Phys.*, 1991, **69**, 4333.
- 11 G. Joshi, H. Lee, Y. Lan, X. Wang, G. Zhu, D. Wang, R. W. Gould, D. C. Cuff, M. Y. Tang, M. S. Dresselhaus, G. Chen and Z. Ren, *Nano Lett.*, 2008, **8**, 4670.
- 12 M. Takeda, T. Fukuda, F. Domingo and T. Miura, *J. Solid State Chem.*, 2004, **177**, 471.
- 13 T. Mori, *J. Appl. Phys.*, 2005, **97**, 093703.
- 14 T. Mori and T. Nishimura, *J. Solid State Chem.*, 2006, **179**, 2908.
- 15 S. Maruyama, Y. Miyazaki, K. Hayashi, T. Kajitani and T. Mori, *Appl. Phys. Lett.*, 2012, **101**, 152101.
- 16 G. A. Slack, D. W. Oliver and F. H. Horn, *Phys. Rev. B*, 1971, **4**, 1714.
- 17 D. G. Cahill, H. E. Fischer, S. K. Watson, R. O. Pohl and G. A. Slack, *Phys. Rev. B*, 1989, **40**, 3254.
- 18 K. Kudou, S. Okada, T. Mori, K. Iizumi, T. Shishido, T. Tanaka, I. Higashi, P. R. K. Nakajima, Y. B. Andersson and T. Lundström, *Jpn. J. Appl. Phys.*, 2002, **41**, 928–930.
- 19 L. F. Wan and S. P. Beckman, *Mater. Lett.*, 2012, **74**, 5.
- 20 H. Werheit, V. Filipov, U. Kuhlmann, U. Schwarz, M. Armbruster, A. Leithe-Jasper, T. Tanaka, I. Higashi, T. Lundstrom, V. N. Gurin and M. M. Korsukova, *Sci. Technol. Adv. Mater.*, 2010, **11**, 023001.
- 21 X. Jiang, J. Zhao, A. Wu, Y. Bai and X. Jiang, *J. Phys.: Condens. Matter*, 2010, **22**, 315503.
- 22 P. Huffman and S. Beckman, *Materials Science and Engineering: A*, 2014, **595**, 266–268.
- 23 L. F. Wan and S. P. Beckman, *Journal of Physics: Condensed Matter*, 2013, **25**, 225502.
- 24 H. Kölpin, D. Music, G. Henkelman and J. M. Schneider, *Phys. Rev. B*, 2008, **78**, 054122.
- 25 L. F. Wan and S. P. Beckman, *IOP Conf. Ser.: Mater. Sci. Eng.*, 2011, **18**, 082024.
- 26 P. Giannozzi and *et al.*, *J. Phys.: Condens. Matter*, 2009, **21**, 395502.
- 27 J. P. Perdew and Y. Wang, *Phys. Rev. B*, 1992, **46**, 12947–12954.
- 28 D. Vanderbilt, *Phys. Rev. B*, 1990, **41**, 7892–7895.
- 29 H. J. Monkhorst and J. D. Pack, *Phys. Rev. B*, 1976, **13**, 5188–5192.
- 30 I. Higashi, *J. Less-Common Met.*, 1981, **82**, 317–323.
- 31 J. M. Ziman, *Principles of the Theory of Solids*, Cambridge University Press, Cambridge, England, 1972.
- 32 P. B. Allen, W. E. Pickett and H. Krakauer, *Phys. Rev. B*, 1988, **37**, 7482.
- 33 G. K. H. Madsen and D. J. Singh, *Comput. Phys. Commun.*, 2006, **175**, 67.
- 34 S. Mezziane, H. Feraoun, T. Ouahrani and C. Esling, *J. Alloy. Compd.*, 2013, **581**, 731–740.
- 35 L. Wan and S. Beckman, *Solid State Sciences*, 2014, under review.
- 36 D. J. Singh, *Recent trends in thermoelectric materials research 2*, Academic Press, 2001, ch. 5, pp. 125–177.
- 37 J. Heyd, G. E. Scuseria and M. Ernzerhof, *J. Chem. Phys.*, 2003, **118**, 8207.
- 38 G. Kresse and J. Furthmüller, *Comput. Mat. Sci.*, 1996, **6**, 15.
- 39 G. Kresse and J. Furthmüller, *Phys. Rev. B*, 1996, **54**, 11169.
- 40 G. Kress and J. Hafner, *J. Phys. Condens. Matter*, 1994, **6**, 8245.
- 41 H. Werheit, U. Kuhlmann, G. Krach, I. Higashi, T. Lundstrom and Y. Y., *J. Alloy Compd.*, 1993, **202**, 269.
- 42 L. Wan and S. Beckman, *Physica B: Condensed Matter*, 2014, **438**, 9–12.
- 43 G. J. Snyder and E. S. Toberer, *Nature Mater.*, 2008, **7**, 105.
- 44 D. R. Clarke, *Surf. Coat. Tech.*, 2003, **163-164**, 67.
- 45 L. F. Wan and S. P. Beckman, *Phys. Rev. Lett.*, 2012, **109**, 145501.
- 46 S. Maruyama, A. Prytuliak, Y. Miyazaki, K. Hayashi, T. Kajitani and T. Mori, *J. Appl. Phys.*, 2014, **115**, 123702.